The influence of Fermi motion on the comparison of the polarization transfer to a proton in elastic e→p and quasi-elastic e→A scattering

(A1 Collaboration) Paul, Sebouh; Brecelj, T.; Arenhövel, H.; Achenbach, P.; Ashkenazi, A.; Beričič, J.; Böhm, R.; Bosnar, Damir; Cohen, E.O.; Debenjak, L.; ...

The influence of Fermi motion on the comparison of the polarization transfer to a proton in elastic $\vec{e}p$ and quasi-elastic $\vec{e}A$ scattering

A1 Collaboration

Sebouh Paul [a,*], T. Brecelj [b], H. Arenhövel [c], P. Achenbach [c], A. Ashkenazi [a], J. Beričič [b],
R. Böhm [c], D. Bosnar [d], E.O. Cohen [a], L. Debenjak [b], M.O. Distler [c], A. Esser [c], I. Friščić [d,1],
R. Gilman [e], D. Izraeli [a], T. Kolar [b], I. Korover [a,f], J. Lichtenstadt [a], I. Mardor [a,g], H. Merkel [c],
D.G. Middleton [c], M. Mihovilovič [b,c,h], U. Müller [c], M. Olivenboim [a], E. Piasetzky [a],
J. Pochodzalla [c], G. Ron [i], B.S. Schlimme [c], M. Schoth [c], F. Schulz [c], C. Sfienti [c], S. Širca [h,b],
S. Štajner [b], S. Strauch [j], M. Thiel [c], A. Tyukin [c], A. Weber [c], I. Yaron [a]

[a] *School of Physics and Astronomy, Tel Aviv University, Tel Aviv 69978, Israel*
[b] *Jožef Stefan Institute, 1000 Ljubljana, Slovenia*
[c] *Institut für Kernphysik, Johannes Gutenberg-Universität, 55099 Mainz, Germany*
[d] *Department of Physics, Faculty of Science, University of Zagreb, HR-10000 Zagreb, Croatia*
[e] *Rutgers, The State University of New Jersey, Piscataway, NJ 08855, USA*
[f] *Department of Physics, NRCN, P.O. Box 9001, Beer-Sheva 84190, Israel*
[g] *Soreq NRC, Yavne 81800, Israel*
[h] *Faculty of Mathematics and Physics, University of Ljubljana, 1000 Ljubljana, Slovenia*
[i] *Racah Institute of Physics, Hebrew University of Jerusalem, Jerusalem 91904, Israel*
[j] *University of South Carolina, Columbia, SC 29208, USA*

ARTICLE INFO

ABSTRACT

A comparison between polarization-transfer to a bound proton in quasi-free kinematics by the $A(\vec{e}, e'\vec{p})$ knockout reaction and that in elastic scattering off a free proton can provide information on the characteristics of the bound proton. In the past the reported measurements have been compared to those of a free proton with zero initial momentum. We introduce, for the first time, expressions for the polarization-transfer components when the proton is initially in motion and compare them to the ^{2}H data measured at the Mainz Microtron (MAMI). We show the ratios of the transverse (P_x) and longitudinal (P_z) components of the polarization transfer in ^{2}H$(\vec{e}, e'\vec{p})$n, to those of elastic scattering off a "moving proton", assuming the proton's initial (Fermi-motion) momentum equals the negative missing momentum in the measured reaction. We found that the correction due to the proton motion is up to 20% at high missing momentum. However the effect on the double ratio $\frac{(P_x/P_z)^A}{(P_x/P_z)^{1_H}}$ is largely canceled out, as shown for both ^{2}H and ^{12}C data. This implies that the difference between the resting- and the moving-proton kinematics is not the primary cause for the deviations between quasi-elastic and elastic scattering reported previously.

1. Introduction

Polarization transfer from a polarized electron to a proton in an elastic scattering reaction has become a recognized method to measure the ratio of the proton's elastic electromagnetic form factors G_E/G_M [1–9]. For a proton initially at rest, assuming the one-photon exchange approximation, the ratio of the transverse (P_x) to longitudinal (P_z) polarization-transfer components, with respect to the momentum transfer $\vec{q}$, is proportional to G_E/G_M [10]:

$$\left(\frac{P_x}{P_z}\right)_H = -\frac{2M}{(k_0 + k'_0)\tan(\theta_{k,k'}/2)}\frac{G_E}{G_M}, \qquad (1)$$

where k_0, k_0' are respectively the initial and final electron energies, $\theta_{k,k'}$ is the electron scattering angle in the lab frame, and M is the proton's mass. This provides a direct measurement of the form factor (FF) ratio and eliminates many systematic uncertainties [11].

Measuring the ratio of the components of the polarization transfer to a knock-out proton in quasi-free kinematics on nuclei, which is sensitive to the electromagnetic FF ratio, has been suggested as a method to study differences between free and bound protons [4,5]. As such it can be used as a tool to identify medium modifications in the bound proton's internal structure [12], reflected in the FFs and thereby in the polarization transfer. Deviations between polarization ratios in quasi-free and elastic scattering can be interpreted only with realistic calculations of the nuclear effects, such as final state interactions (FSI), meson exchange currents (MEC), isobar currents (IC), and relativistic corrections on the outgoing proton polarization components [13–15]. However, a comparison to the polarization transfer on a free proton should also consider the Fermi motion of the struck proton, rather than comparing to a reaction with the proton at rest.

Polarization-transfer experiments have been carried out recently on ^{2}H and ^{12}C target nuclei at the Mainz Microtron (MAMI) [13,14,16], as well as on ^{2}H, ^{4}He and ^{16}O at Jefferson Lab [17–21], in search of medium modification in the bound proton's internal structure. In particular, these experiments were performed to study deeply bound nucleons, characterized by high missing momentum, which is equivalent (neglecting FSI) to protons with high initial momentum. It was shown in [13,14] that for ^{2}H at low momentum transfer,[2] the deviations can be explained by nuclear effects without the necessity of introducing modified FFs. In these experiments, the comparison to the free proton was done either by measurements of the polarization transfer ratio to ^{1}H at similar kinematics [17,18], or by calculations using Eq. (1) and a fit to the world data of proton FFs [11,22], which were used in [13,14,16].

Kinematically, quasi-elastic scattering differs from elastic scattering in that the bound proton is *off*-shell, and in that it moves relative to the nucleus with Fermi motion. However, using Eq. (1) to calculate the polarization ratio is only valid if the proton is both *on*-shell and at rest.

In this work we introduce an alternative approach: comparing the polarization transfer in quasi-free scattering to that of a free proton (on-shell) with a finite initial momentum. The general expressions for polarization transfer to a free moving proton have been developed. We applied this prescription to the ^{2}H and ^{12}C data measured at MAMI over relatively large missing momentum ranges. The elastic kinematics are described in Section 2, while the polarization transfer formulae are given in Section 3. The application of this prescription to MAMI data is shown in Section 4.

2. Kinematics

The kinematics are defined by an electron with initial four-momentum k scattering off a proton with initial four-momentum p, through exchange of a virtual photon with four-momentum q, resulting in the two particles having final four-momenta k' and p' respectively.

The final momenta of the proton and electron, $\vec{p}\,'$ and $\vec{k}\,'$, are measured in the spectrometers. The "missing momentum", defined as $\vec{p}_{\text{miss}} = \vec{q} - \vec{p}\,'$, is calculated using the momentum transfer defined by $\vec{q} = \vec{k} - \vec{k}\,'$. In the absence of FSI, the initial proton momentum is given by the missing momentum, $\vec{p} = -\vec{p}_{\text{miss}}$. By convention, the missing momentum is considered positive (negative) if $\vec{p}_{\text{miss}} \cdot \vec{q}$ is positive (negative).
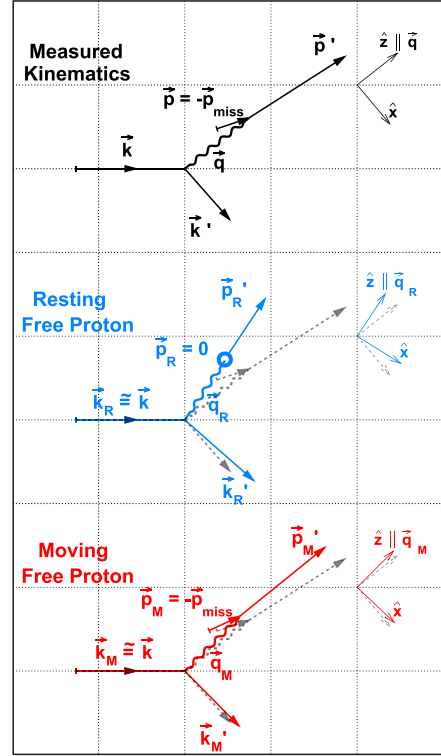
Fig. 1. The measured kinematics for a sample QE event (top) compared to the resting (middle) and moving (bottom) elastic kinematics. In the middle and bottom plots, the solid lines show the free-proton kinematics and the dashed lines show the measured kinematics. In the middle plot, the initial momentum of the proton is zero. In the bottom plot, the proton's initial momentum is the negative missing momentum, which neglecting FSI, is equal to the bound proton's initial momentum $\vec{p}$ in the top plot. The transformation from the measured kinematics to the moving free-proton kinematics causes smaller changes to the magnitudes of the vectors $\vec{k}$, $\vec{k}\,'$, $\vec{q}$ and $\vec{p}\,'$, and the angles between them, than the transformation to resting free-proton kinematics.

These measured kinematics are shown in the top diagram in Fig. 1, and are compared, in the middle and bottom diagrams, to the kinematics of elastic scattering off a proton initially at rest, and off a proton with initial momentum $\vec{p} = -\vec{p}_{\text{miss}}$, respectively.

Each measured quasi-elastic event is compared to an elastic event that has the same incident energy (k_0), the same magnitude of the four-momentum transfer ($Q^2 = -q^2$) and the same initial proton momentum ($\vec{p}$) as the measured quasi-elastic event. Also, the struck proton is on-shell in its initial and final state in the elastic event.[3] These criteria uniquely define a set of kinematics, here referred to as "moving-proton" kinematics. We use a subscript "$_M$" to distinguish between the kinematic variables in the moving-proton kinematics from the measured quantities.

In the standard coordinate system for polarization transfer, where $\vec{q} \parallel \hat{z}$ and the scattering is in the xz plane, the moving-proton kinematics are[4]:

$$p_M = \left(p_{0M}, \, p_x, \, p_y, \, p_z \right), \tag{2}$$

$$k_M = \left(k_0, \, \frac{Q\sqrt{4k_0(k_0 - \omega_M) - Q^2}}{2q_{zM}}, \, 0, \, \frac{2k_0\omega_M + Q^2}{2q_{zM}} \right), \tag{3}$$

$$p_M' = p_M + q_M, \tag{4}$$

and

---

[2] These data were taken at $Q^2 = 0.18$ and 0.4 (GeV/c)^2.

[3] This is equivalent to the Bjorken condition, $\left[\frac{Q^2}{2p \cdot q} \right]_M = 1$.

[4] For the derivation, see the supplementary material.

$$k'_M = k_M - q_M, \tag{5}$$

where

$$q_M = (\omega_M, \ 0, \ 0, \ q_{zM}), \tag{6}$$

$$\omega_M = \frac{Q^2 p_{0M} + p_z Q \sqrt{4E_{pt}^2 + Q^2}}{2E_{pt}^2}, \tag{7}$$

and

$$q_{zM} = \sqrt{Q^2 + \omega_M^2}, \tag{8}$$

using p_{0M} and E_{pt} as shorthand for $\sqrt{M^2 + |\vec{p}|^2}$ and $\sqrt{M^2 + p_x^2 + p_y^2}$, respectively. Note that p_x, p_y and p_z are the co-ordinates of $\vec{p} = -\vec{p}_{\text{miss}}$ in the $\vec{q} \, || \, \hat{z}$ coordinate system.

In previous publications [13,14,16], we used a different type of free-proton kinematics ("resting proton", denoted with a subscript "$_R$" in Fig. 1 and elsewhere in this paper) where instead of having the same $\vec{p}$ as in the measured kinematics, we had $\vec{p}_R = \vec{0}$. The resting-proton kinematics may therefore be evaluated by substituting $\vec{p} = 0$ in Eqs. (2)–(8).

3. Polarization transfer

The general expressions for the polarization transfer from a longitudinally polarized electron to an initially moving nucleon with momentum $\vec{p}$ in the scattering plane are presented below, with more details in [23]:

$$P_x = -C_P G_M \left(G_E(\alpha_{\ell x} - \beta_{\ell x}) + G_M \beta_{\ell x} \right), \tag{9}$$

$$P_z = -C_P G_M \left(G_E(\alpha_{\ell z} - \beta_{\ell z}) + G_M \beta_{\ell z} \right), \tag{10}$$

where

$$C_P = \frac{2}{(1 + \tau) M^2 \Sigma_0}, \tag{11}$$

$$\Sigma_0 = (G_E^2 + \tau G_M^2) \left(\frac{(K \cdot p)^2}{M^2 Q^2 (1 + \tau)} - 1 \right) + 2\tau G_M^2, \tag{12}$$

$$\alpha_{\ell x} = \frac{1 + \tau}{2} \left(\frac{p_x}{p_0' + M} \left(M K_0 + 2p \cdot k - \frac{Q^2}{2} \right) - M K_x \right), \tag{13}$$

$$\beta_{\ell x} = \frac{-1}{4M^2} \left(2k \cdot p - \frac{Q^2}{2} \right) \frac{p_x}{p_0' + M} \left(M\omega - \frac{Q^2}{2} \right), \tag{14}$$

$$\alpha_{\ell z} = \frac{1 + \tau}{2} \left(\frac{p_z + q_z}{p_0' + M} \left(M K_0 + 2p \cdot k - \frac{Q^2}{2} \right) - M K_z \right), \tag{15}$$
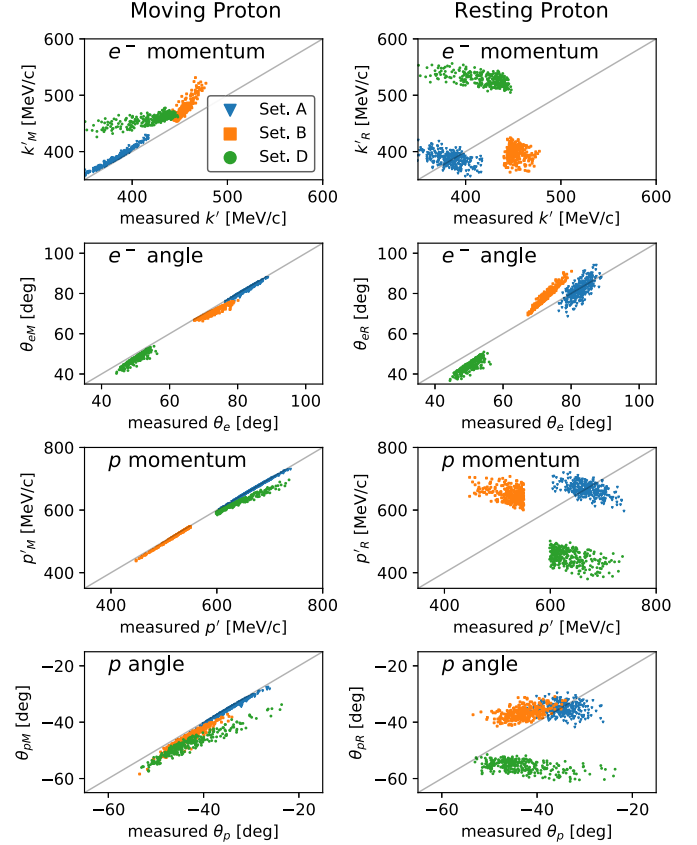
and

$$\beta_{\ell z} = \frac{-1}{4M^2} \left(2k \cdot p - \frac{Q^2}{2} \right) \left(\frac{p_z + q_z}{p_0' + M} \left(M\omega - \frac{Q^2}{2} \right) - M q_z \right), \tag{16}$$

using $\tau = \frac{Q^2}{4M^2}$ and $K = k + k'$. The factors of $-C_P G_M$ in Eq. (9) and (10) cancel out in the ratio:

$$\frac{P_x}{P_z} = \frac{G_E(\alpha_{\ell x} - \beta_{\ell x}) + G_M \beta_{\ell x}}{G_E(\alpha_{\ell z} - \beta_{\ell z}) + G_M \beta_{\ell z}}. \tag{17}$$

Equation (17) reduces to Equation (1) if the proton is initially at rest. It should be noted that the formulae in this section are only valid for *elastic* scattering in the one-photon approximation.

Fig. 2. Comparison of the kinematic variables measured for ^{2}H in [13,14] (x-axis) to those in the moving-proton (left) and resting-proton (right) prescriptions (y-axis). The different colors represent different kinematic settings. The variables, from top to bottom, are the momentum and angle of the scattered electron (k' and θ_e), and those of the recoiling proton (p' and θ_p). The two angles are measured relative to the beam $\vec{k}$. These variables were selected because they are the ones that are directly measured in the experiment.

4. Application to MAMI A($\vec{e}, e'\vec{p}$) data

Polarization-transfer measurements on ^{2}H and ^{12}C have been carried out at MAMI [24,25] at momentum transfers of $Q^2 = 0.18$ and 0.40 (GeV/c)^2 [13,14,16]. The kinematic settings of the measurements are given in Tables 1 and 2 of the supplemental material. The double ratios $\frac{(P_x/P_z)^A}{(P_x/P_z)^{^1\text{H}}}$ were presented for both nuclei as functions of the struck proton's virtuality ("off-shellness"), $\nu \equiv (p' - q)^2 - M^2$, which proved to be a useful parameter for a unified description of the deviation of the bound proton from a free one. In addition, Ref. [14] presents the ratios $\frac{(P_x)^A}{(P_x)^{^1\text{H}}}$ and $\frac{(P_z)^A}{(P_z)^{^1\text{H}}}$ for the deuteron data, and showed that they were in agreement with the theoretical calculation, indicating that the deviations from the free proton were primarily due to FSI.

Applying the moving-proton prescription to the deuteron data [13,14], we notice a good correspondence between the measured and evaluated kinematic variables in the left side of Fig. 2. These differences are much smaller than those between the *resting*-proton kinematics and the measured kinematics, shown on the right side of Fig. 2.

The differences between the measured and the resting-proton kinematics are more pronounced for settings B and D than in setting A, due to larger $|\vec{p}_{\text{miss}}|$ and virtuality in the former.

There are larger differences between the moving-proton kinematics and the measured kinematics in the ^{12}C data [16], as shown
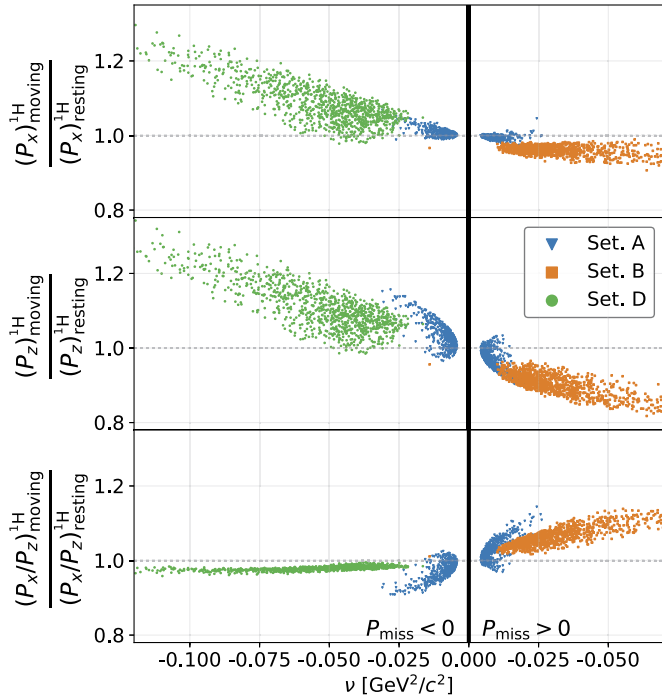
Fig. 3. Ratios of P_x, P_z and P_x/P_z for moving free protons to those for free resting protons, using the kinematics derived from measured events in $^2\mathrm{H}(\vec{e}, e'\vec{p})$n reactions reported in [14]. Different colors represent different kinematic setups. See [13, 14] for details.

in the supplementary material, due to the larger Fermi motion in the carbon nucleus. However, they are still much smaller than the difference between the resting-proton kinematics and the measured kinematics.

In Fig. 3, we compare the polarization-transfer components calculated for the resting- and the moving-proton kinematics. We show in this figure the ratios $(P_x)^{1\mathrm{H}}_{\mathrm{moving}}/(P_x)^{1\mathrm{H}}_{\mathrm{resting}}$, $(P_z)^{1\mathrm{H}}_{\mathrm{moving}}/(P_z)^{1\mathrm{H}}_{\mathrm{resting}}$, and $(P_x/P_z)^{1\mathrm{H}}_{\mathrm{moving}}/(P_x/P_z)^{1\mathrm{H}}_{\mathrm{resting}}$, as calculated for the kinematics of the $^2\mathrm{H}$ events in Ref. [13]. The difference between resting and moving for the individual components is small around $\nu = 0$, and it increases up to 20% (15%) at large virtuality[5] with negative (positive) p_{miss}. The difference between moving and resting in the ratio P_x/P_z is small: up to 3% for $p_{\mathrm{miss}} < 0$ and up to 10% at $p_{\mathrm{miss}} > 0$.

The ratios of the polarization observables measured for the deuteron to the values calculated event-by-event for a moving proton using Equations (9) and (10) are shown in Fig. 4. These are contrasted with the corresponding ratios for the resting proton, which were reported in [14]. The double ratio $\frac{(P_x/P_z)^{2\mathrm{H}}}{(P_x/P_z)^{1\mathrm{H}}}$, calculated event-by-event, is also presented in Fig. 4, using a procedure described in detail in the supplementary material. As expected from Fig. 3, the moving effect on the double ratio is small.

A good agreement was found between the double ratios $\frac{(P_x/P_z)^A}{(P_x/P_z)^{1\mathrm{H}}}$ measured for $^{12}\mathrm{C}$ and $^2\mathrm{H}$ as functions of virtuality using resting-proton kinematics [16]. In order to test if this agreement is preserved using *moving*-proton kinematics, we calculated the double ratios for the $^{12}\mathrm{C}$ datasets from MAMI [16] in the same manner as for $^2\mathrm{H}$. The double ratios for the two nuclei are compared with
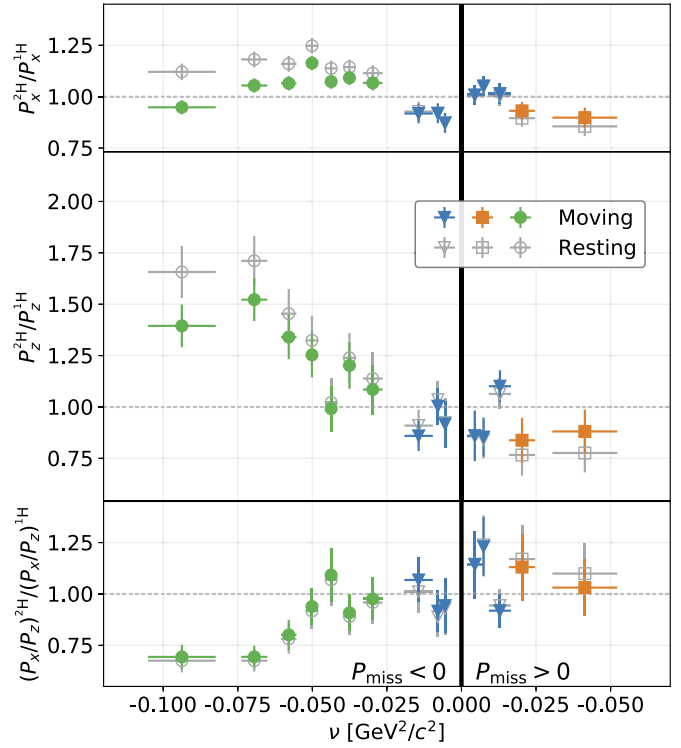
Fig. 4. The measured ratios, $(P_x)^{2\mathrm{H}}/(P_x)^{1\mathrm{H}}$ and $(P_z)^{2\mathrm{H}}/(P_z)^{1\mathrm{H}}$ and the double ratio $(P_x/P_z)^{2\mathrm{H}}/(P_x/P_z)^{1\mathrm{H}}$, using *moving* free-proton in the denominator are shown as functions of the proton virtuality, ν (filled colored symbols). These are compared to the same ratios with *resting* free-proton kinematics (grey open symbols) from [14]. The virtuality dependence is shown separately for positive and negative missing momenta. The different symbols and colors for the data of this work correspond to the different kinematical settings.
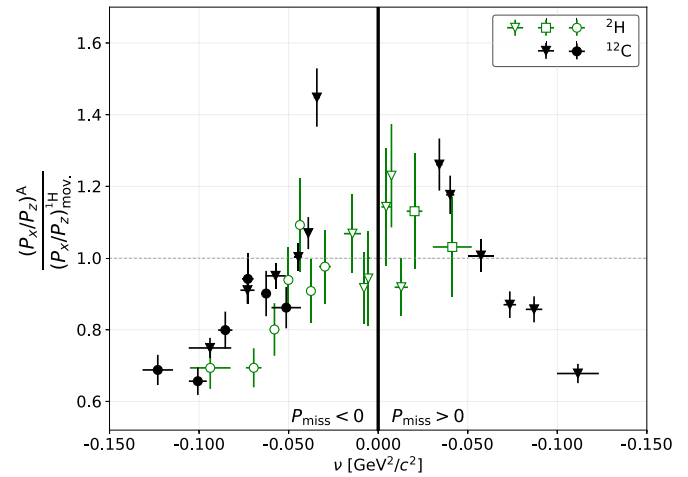
Fig. 5. The measured double ratios $(P_x/P_z)^A/(P_x/P_z)^{1\mathrm{H}}$, using moving free-proton kinematics in the denominator, are shown as functions of the proton virtuality, for both $^{12}\mathrm{C}$ and $^2\mathrm{H}$. (The large double-ratios for carbon at $|\nu| < 0.04$ GeV$^2/c^2$ have been attributed [16] to knock-out of $p_{3/2}$-shell protons at small $|p_{\mathrm{miss}}|$ [26–28].)

one another in Fig. 5, showing that the good agreement is maintained.

5. Conclusions

We observe that using the moving-proton kinematics described in this paper reduces, but does not eliminate, the difference between measured components of the polarization transfer in quasi-

---

[5] This is expected, since the $|\vec{p}_{\mathrm{miss}}|$ is near zero at small ν and increases monotonically with ν for any given target and residual nuclear masses.

free scattering and those in elastic scattering. The deviations from the free-proton in the transverse (P_x) component become smaller (around 7%) when using the moving kinematics. Similarly, the deviations in the longitudinal (P_z) component are reduced, but remain significantly large, up to 50% (Fig. 4). Since using the moving proton kinematics has a similar effect on both components, the effect on the double ratio largely cancels out. Thus the double ratio is less sensitive to the kinematics than the separate components. This implies that the choice of elastic kinematics is not the primary cause of the deviations in P_x/P_z between quasi-free and elastic scattering.

It was previously noted that the virtuality is a useful parameter for comparing the double ratio $\frac{(P_x/P_z)^A}{(P_x/P_z)^{1\mathrm{H}}}$ of different nuclei at different Q^2. Here we show that the double ratio has only a weak sensitivity to the initial momentum of the proton, which continues to make the double ratio a preferred observable for studying the differences between bound and free protons.

Acknowledgements

Appendix A. Supplementary material

Supplementary material related to this article can be found online at https://doi.org/10.1016/j.physletb.2019.04.004.

References

[1] M.K. Jones, et al., G_{Ep}/G_{Mp} ratio by polarization transfer in polarized $\vec{e}p \rightarrow e\vec{p}$, Phys. Rev. Lett. 84 (2000) 1398–1402, https://doi.org/10.1103/PhysRevLett.84.1398.

[2] O. Gayou, et al., Measurement of G_{Ep}/G_{Mp} in $\vec{e}p \rightarrow e\vec{p}$ to $Q^2 = 5.6$ GeV^2, Phys. Rev. Lett. 88 (2002) 092301, https://doi.org/10.1103/PhysRevLett.88.092301, arXiv:nucl-ex/0111010.

[3] V. Punjabi, et al., Proton elastic form-factor ratios to Q^2 = 3.5 GeV^2 by polarization transfer, Phys. Rev. C 71 (2005) 055202, https://doi.org/10.1103/PhysRevC.71.055202, arXiv:nucl-ex/0501018; Erratum: Phys. Rev. C 71 (2005) 069902.

[4] B.D. Milbrath, et al., A comparison of polarization observables in electron scattering from the proton and deuteron, Phys. Rev. Lett. 80 (1998) 452–455, https://doi.org/10.1103/PhysRevLett.80.452, arXiv:nucl-ex/9712006; Erratum: Phys. Rev. Lett. 82 (1999) 2221.

[5] D.H. Barkhuff, et al., Measurement of recoil proton polarizations in the electrodisintegration of deuterium by polarized electrons, Phys. Lett. B 470 (1999) 39–44, https://doi.org/10.1016/S0370-2693(99)01294-0.

[6] T. Pospischil, et al., Measurement of G_{Ep}/G_{Mp} via polarization transfer at $Q^2 = 0.4$ (GeV/$c)^2$, Eur. Phys. J. A 12 (2001) 125–127, https://doi.org/10.1007/s100500170046.

[7] O. Gayou, K. Wijesooriya, et al., Measurements of the elastic electromagnetic form factor ratio $\mu_p G_{ep}/G_{mp}$ via polarization transfer, Phys. Rev. C 64 (2001) 038202, https://doi.org/10.1103/PhysRevC.64.038202.

[8] G. MacLachlan, et al., The ratio of proton electromagnetic form factors via recoil polarimetry at $Q^2 = 1.13$ (GeV/$c)^2$, Nucl. Phys. A 764 (2006) 261–273, https://doi.org/10.1016/j.nuclphysa.2005.09.012.

[9] M.K. Jones, et al., Proton G_E/G_M from beam-target asymmetry, Phys. Rev. C 74 (2006) 035201, https://doi.org/10.1103/PhysRevC.74.035201.

[10] A.I. Akhiezer, M. Rekalo, Polarization effects in the scattering of leptons by hadrons, Sov. J. Part. Nucl. 4 (1974) 277, Fiz. Elem. Chast. Atom. Yadra 4 (1973) 662.

[11] C.F. Perdrisat, et al., Nucleon electromagnetic form factors, Prog. Part. Nucl. Phys. 59 (2007) 694–764, https://doi.org/10.1016/j.ppnp.2007.05.001.

[12] M.M. Sargsian, et al., Hadrons in the nuclear medium, J. Phys. G 29 (2003) R1, https://doi.org/10.1088/0954-3899/29/3/201.

[13] I. Yaron, D. Izraeli, et al., Polarization-transfer measurement to a large-virtuality bound proton in the deuteron, Phys. Lett. B 769 (2017) 21–24, https://doi.org/10.1016/j.physletb.2017.01.034.

[14] D. Izraeli, I. Yaron, et al., Components of polarization-transfer to a bound proton in a deuteron measured by quasi-elastic electron scattering, Phys. Lett. B 781 (2018) 107–111, https://doi.org/10.1016/j.physletb.2018.03.063, arXiv:1801.01306.

[15] H. Arenhövel, W. Leidemann, E.L. Tomusiak, General survey of polarization observables in deuteron electrodisintegration, Eur. Phys. J. A 23 (2005) 147–190, https://doi.org/10.1140/epja/i2004-10061-5.

[16] D. Izraeli, T. Brecelj, et al., Measurement of polarization-transfer to bound protons in carbon and its virtuality dependence, Phys. Lett. B 781 (2018) 95–98, https://doi.org/10.1016/j.physletb.2018.03.027, arXiv:1711.09680.

[17] B. Hu, et al., Polarization transfer in the ^{2}H($\vec{e}, e'\vec{p}$)n reaction up to $Q^2 = 1.61$ (GeV/$c)^2$, Phys. Rev. C 73 (2006) 064004, https://doi.org/10.1103/PhysRevC.73.064004.

[18] S. Strauch, et al., Polarization transfer in the ^{4}He($\vec{e}, e'\vec{p}$)^{3}H reaction up to $Q^2 = 2.6$ (GeV/$c)^2$, Phys. Rev. Lett. 91 (2003) 052301, https://doi.org/10.1103/PhysRevLett.91.052301.

[19] M. Paolone, S.P. Malace, S. Strauch, et al., Polarization transfer in the ^{4}He($\vec{e}, e'\vec{p}$)^3**H** reaction at $Q^2 = 0.8$ and 1.3 (GeV/$c)^2$, Phys. Rev. Lett. 105 (2010) 072001, https://doi.org/10.1103/PhysRevLett.105.072001.

[20] S. Dieterich, et al., Polarization transfer in the ^{4}He($\vec{e}, e'\vec{p}$)^{3}H reaction, Phys. Lett. B 500 (1–2) (2001) 47–52, https://doi.org/10.1016/S0370-2693(01)00052-1.

[21] S. Malov, et al., Polarization transfer in the ^{16}O($\vec{e}, e'\vec{p}$)^{15}N reaction, Phys. Rev. C 62 (2000) 057302, https://doi.org/10.1103/PhysRevC.62.057302.

[22] J.C. Bernauer, et al., Electric and magnetic form factors of the proton, Phys. Rev. C 90 (1) (2014) 015206, https://doi.org/10.1103/PhysRevC.90.015206.

[23] H. Arenhövel, et al., Polarization observables for elastic electron scattering off a moving nucleon, Phys. Rev. C (2019), in press, arXiv:1904.04515.

[24] K. Blomqvist, et al., The three-spectrometer facility at MAMI, Nucl. Instrum. Methods, Sect. A 403 (2–3) (1998) 263–301, https://doi.org/10.1016/S0168-9002(97)01133-9.

[25] T. Pospischil, et al., The focal plane proton-polarimeter for the 3-spectrometer setup at MAMI, Nucl. Instrum. Methods Phys. Res., Sect. A 483 (3) (2002) 713–725, https://doi.org/10.1016/S0168-9002(01)01955-6.

[26] J. Ryckebusch, D. Debruyne, W. Van Nespen, S. Janssen, Meson and isobar degrees of freedom in $(\vec{e}, e'\vec{p})$ reactions at $0.2 < Q^2 < 0.8$ (GeV/$c)^2$, Phys. Rev. C 60 (1999) 034604, https://doi.org/10.1103/PhysRevC.60.034604.

[27] C. Giusti, J. Ryckebusch, private communication, 2017.

[28] D. Dutta, et al., Quasielastic ($e, e'p$) reaction on ^{12}C, ^{56}Fe, and ^{197}Au, Phys. Rev. C 68 (2003) 064603, https://doi.org/10.1103/PhysRevC.68.064603.